PROCEEDINGS OF SCIENCE

Search for cosmic neutrino point sources and extended sources with 6-21 lines of KM3NeT/ARCA

Rasa Muller,[a,*] **Thijs van Eeden**[a] **and Aart Heijboer**[a] **on behalf of the KM3NeT Collaboration**

[a] *Nikhef, Science Park 105, Amsterdam, Netherlands*

E-mail: rmuller@km3net.de, aart.heijboer@nikhef.nl, tjuanve@nikhef.nl

The identification of cosmic objects emitting high energy neutrinos provides new insights about the Universe and its active sources. The existence of cosmic neutrinos has been proven by the IceCube Neutrino Observatory, but the big question of which sources these neutrinos originate from remains largely unanswered. The KM3NeT detector for Astroparticle Research with Cosmics in the Abyss (ARCA), is currently being built in the Mediterranean Sea. It will have an instrumented volume of a cubic kilometre, and excel at identifying cosmic neutrino sources due to its unprecedented angular resolution (< 0.1 degree for muon neutrinos with E > 100 TeV). KM3NeT has a view of the sky complementary to IceCube, and is sensitive to neutrinos across a wide range of energies. Currently KM3NeT/ARCA is taking data with 21 detector lines. This contribution will present the results of point source and extended source searches with KM3NeT/ARCA with data from 2021 and 2022 taken with an evolving detector geometry.

PoS(ICRC2023)1018

38th International Cosmic Ray Conference (ICRC2023)
26 July - 3 August, 2023
Nagoya, Japan

ICRC2023 38th International Cosmic Ray Conference The Astroparticle Physics Conference

*Speaker

1. Introduction

IceCube has identified TXS 0506+056 as a flaring neutrino source [1–3] and has recently identified NGC 1068 as a steady point source of high energy neutrinos (4.2σ) [4] (November 4th, 2022). In their respective energy ranges the sources NGC 1068 and TXS 0506+056 contribute no more than $\sim 1\%$ to the overall diffuse flux of astrophysical neutrinos. This indicates that there is still a lot of work to be done in identifying the sources that produce high energy neutrinos. This is where KM3NeT/ARCA will play an important role.

The KM3NeT/ARCA detector is a neutrino telescope currently under construction at the bottom of the Mediterranean Sea. It consists of a three-dimensional grid of optical modules that detect the Cherenkov light from neutrino interaction products. The full detector will have 230 detection lines of 18 optical modules and will instrument ~ 1 km^3 volume of sea water.

For 101 astrophysical objects it is tested whether they are high energy neutrino emitters. In order to identify a cosmic neutrino signal on top of the atmospheric background of muons and neutrinos, statistical methods are developed based on Monte Carlo pseudo experiments. With the KM3NeT/ARCA data taken with 6, 8, 19, and 21 detection units, the expected sensitivity of KM3NeT/ARCA to neutrino point and extended sources in our universe is calculated in a binned likelihood analyses. The methods and results are presented in this contribution.

2. KM3NeT/ARCA6-21 data and performance

2.1 Data sample

This analysis uses data from a period when KM3NeT/ARCA was running with 6 - 21 detector strings between May 2021, and December 2022. The effective data taking time of $\sim$ 424 days contains: $\sim$ 92 days with 6 lines (referred to as ARCA6), $\sim$ 210 days with 7 - 8 lines (referred to as ARCA8), $\sim$ 52 days with ARCA19 and $\sim$ 69 days with ARCA21. The different periods have been studied individually, but unless stated differently, the plots shown in this contribution include the full period.

2.2 Background rejection, event selection

The event selection criteria are applied to reduce the atmospheric muon contamination and discard badly reconstructed events. Events are selected using cuts on the number of hits used in the reconstruction, the reconstructed direction, and the fit quality, which is based on the likelihood of the reconstruction. For the ARCA19-21 period an additional boosted decision tree model is trained to further discriminate signal from background.

The selection efficiencies for ν_μ CC track events reconstructed within $1°$ from the true neutrino direction is 81% for the ARCA6-8 period and 95% for the ARCA19-21 period. A cosmic flux of $\phi^{\cos}_{\nu_i+\bar{\nu}_i} = 1.2 \cdot 10^{-8} \left(\frac{E_\nu}{\mathrm{GeV}}\right)^{-2}$ GeV^{-1} cm^{-2} s^{-1} sr^{-1} yields 16.5 events in the ARCA6-21 data sample.

In Figure 1, the reconstructed energy distribution of the event samples are shown for the ARCA6-8 and ARCA19-21 periods. There is a 13% overall underestimation of the data by the simulation, but this effect does not affect the analysis since the background estimation comes from scrambled data. As it can be seen in Figure 1 (left), the ARCA6-8 is still dominated by badly reconstructed atmospheric muons, while the ARCA19-21 sample has a higher neutrino purity (Figure 1 - right). It can be explained by the different size of the 2 detectors.

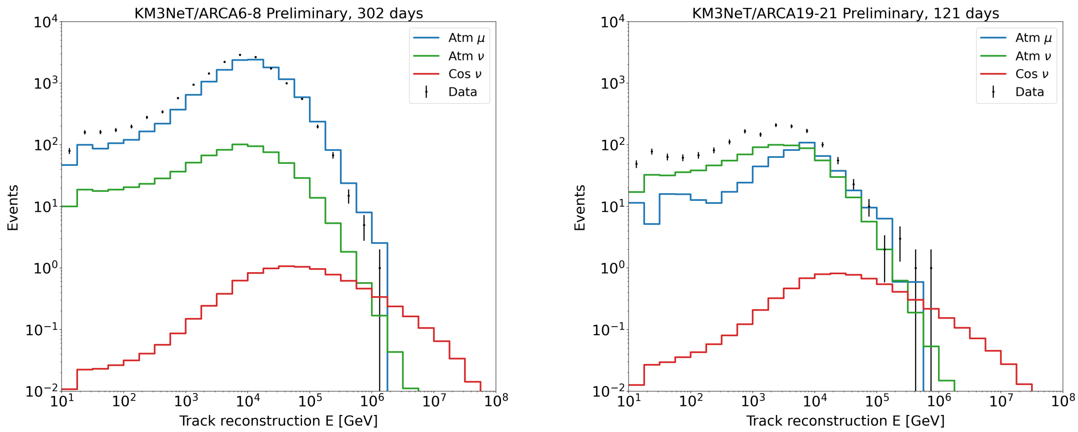

Figure 1: Reconstructed energy distributions after applying the event selections for the ARCA6-8 (left) and ARCA19-21 (right) period.

2.3 Background expectation from scrambled data

The background rate, as a function of reconstructed energy and declination (δ), is data-driven. For the $\sin(\delta)$ a spline $F(\delta)$ is fitted, and the energy dependence $F(\log_{10}(E))$ is parameterised by a fit with two Gaussians. For each individual candidate source that is studied, the expected density of background events in sr^{-1} $\log_{10}(\text{GeV})^{-1}$ is obtained by:

$$N_{\text{bkg}} = n \times F(\delta) \times F(\log_{10}(E)) \tag{1}$$

where the normalisation n is chosen such that the integral over the full solid angle of the sky and over E gives exactly the total number of events in the data.

2.4 Detector response from Monte Carlo simulations

The response of the detector to a possible signal is modeled via detector response functions (acceptance, and resolutions), which are based on simulations [5–7]. Figure 2 (left) shows the effective area of ARCA6-21 compared with ANTARES for similar - yet not exactly the same - event selection, and the angular deviation (right) for selected track events from ν_μ CC interactions for the ARCA6-8 and ARCA19-21 periods. The ARCA6-8 period reaches an angular deviation of $\sim 1°$ at 100 PeV while the ARCA19-21 period already reaches $0.2°$. For the full detector this is expected to improve towards $0.06°$ [8].

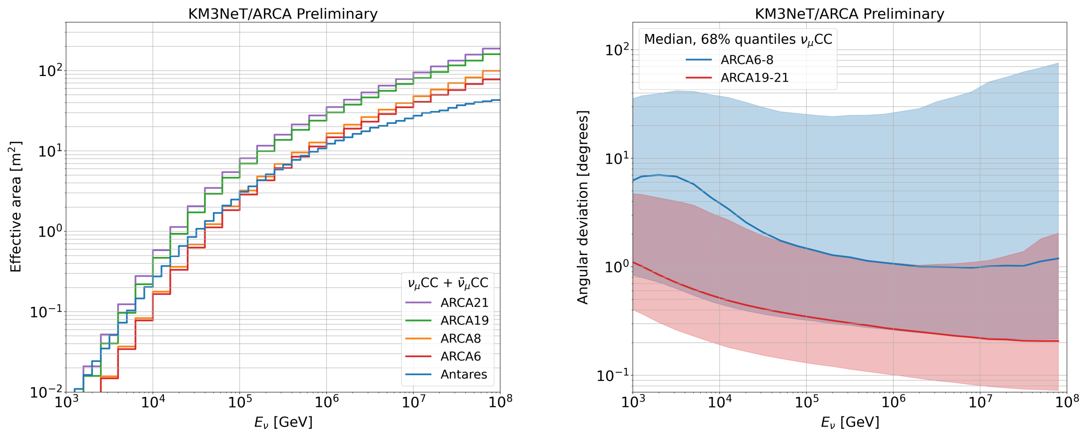

Figure 2: Effective area at selection level (left) for the different ARCA detectors for a flux of $\nu_\mu + \bar{\nu}_\mu$ that interact in the CC interaction. The effective areas are compared with the ANTARES effective area for upgoing events. The angular deviation (right) for the ARCA6-8 and ARCA19-21 periods with their corresponding 68% quantiles.

3. Method

3.1 Candidate sources

The 101 astrophysical objects[1], are selected based on GeV – PeV information from other neutrino experiments, cosmic ray experiments as well as electromagnetic measurements. Besides adding interesting sources from previous point source studies and real time alerts by IceCube and ANTARES, historically interesting sources were added as well as high-energy γ-ray source by the LHAASOO collaboration. Furthermore the γ-ray TeVCat is consulted to select interesting Galactic sources with a hint for a hadronic component, and active galactic nuclei were selected based on their maximal flux observed in radio. For the 10% of sources that are spatially extended in the sky, the detector point spread function is modified with a Gaussian with the spread (σ) equal to the corresponding extension ranging from 0.11 to 1 degrees.

3.2 Analysis method

A binned formalism is used where the compatibility of the data with a point source hypothesis is tested by means of 2D histograms of distance to the candidate source ψ in the range $[0-5]$ in degrees, v.s. $\log_{10}(E_{\mathrm{rec}})$ in the range $[1-8]$, in $\log_{10}(\mathrm{GeV})$. For each bin i, there is an estimate of the number of signal events, $\mathcal{S}_i$, expected for a reference flux ϕ_{ref} and the number of background events, $\mathcal{B}_i$.

[1] The 101 analysed candidates are:
LMC N132D, HESS J1356-645 , SNR G318.2+00.1, IC-hotspot South hemisphere, HESS J1614-518, PKS 2005-489, HESS J1640-465, RX J0852.0-4622, HESS J1641-463, VelaX , PKS 0537-441, CentaurusA, PKS 1424-418, J0106-4034, RX J1713.7-3946, CTB 37A, PKS 1454-354, HESS J1741-302, J1924-2914, Galactic center, J2258-2758, J1625-2527, NGC 253, J0457-2324, J1833-210A, J0836-2016, J1911-2006, J0609-1542, SNR G015.4+00.1, J2158-1501, LHAASO J1825-1326 , QSO 1730-130, J1337-1257, J2246-1206, PKS 0727-11, TXS 1749-101, HESS J1828-099, J1512-0905, J0607-0834, QSO 2022-077, RS Ophiuchi, J0006-0623, 3C279, LHAASO J1839-0545 , J2225-0457, 4FGL J0307.8-0419, PKS 1741-038, LHAASO J1843-0338 , J0339-0146, J0423-0120, J0725-0054, LHAASO J1849-0003 , NGC 1068, J2136+0041, J1058+0133, J0108+0135, PKS 0215+015, J1229+0203, TXS 0310+022, 3C403, CGCG 420-01, J0433+0521, TXS 0506+056, HESS J0632+057, LHAASO J1908+0621 , PKS 2145+067, W 49B, OT 081, PKS 1502+106, J0242+1101, J2232+1143, J0121+1149, J1230+1223, J0750+1231, PKS 1413+135, J0530+1331, W 51, J2253+1608, PKS 0735+178, LHAASO J1929+1745 , J0854+2006, RGB J2243+203, LHAASO J0534+2202 , IC 443, PKS 1424+240, MG3 J225517+2409, 2HWC J1949+244, LHAASO J1956+2845 , J0237+2848, J1310+3220, J1613+3412, LHAASO J2018+3651 , J2015+3710, MGRO J2019+37, Mkn 421, J0927+3902, NGC 4151, Mkn 501, J1642+3948, J0555+3948, LHAASO J2032+41025.

The analysis is done for spectral index $\gamma = 2$ and 2.5. Furthermore a spectrum in line with the most recent NGC 1068 IceCube observation [4] ($\gamma = 3.2$) is tested for this particular source, and this particular source only.

3.2.1 Likelihood formalism

For every (pseudo) dataset it is determined how compatible it is with the expected signal + background model (H1), and with the background-only model (H0). This is expressed in the log-likelihood ratio (λ) which serves as a test statistic:

$$\lambda = \log L(\mu = \hat{\mu}) - \log L(\mu = 0) \tag{2}$$

$$\log L = \sum_{i \in \text{bins}} N_i \log(\mathcal{B}_i + \mu \mathcal{S}_i) - \mathcal{B}_i - \mu \mathcal{S}_i. \tag{3}$$

where μ represents the signal strength and $\hat{\mu}$ the best fitted signal strength for a given (pseudo) dataset.

3.3 Systematic uncertainties

Systematic uncertainties are taken into account for two main parameters describing the detector performance: the angular resolution (0.5° Gaussian smearing) and the acceptance (30% Gaussian spread). The systematic uncertainty on the estimated angular deviation comes from the uncertainty on the absolute orientation of the detector around its z-axis and uncertainty on the tilts of the lines. The uncertainty on the acceptance takes into account the uncertainties on the water and PMT properties. They have been studied in detail in [9, 10].

3.4 Discovery potential and sensitivity

The sensitivity and discovery potential is obtained for a range of declinations with 50.000 pseudo-experiments for the H0 distribution, and 5000 pseudo-experiments for each H1 distribution. Table 1 summarises the results for the E^{-2} and $E^{-2.5}$ spectra. For each of the candidate sources, the discovery potential and sensitivity are calculated with 30.000 pseudo-experiments for the H0 distribution, and 3000 pseudo-experiments for each H1 distribution. Depending on the declination, the sensitivity is at a flux level that would produce 2.2 – 3.2 (for an E^{-2} spectrum), 2.4 – 3.6 (for an $E^{-2.5}$ spectrum) signal events per source in the full data taking period. A discovery would require 1.5 – 4.0 (for an E^{-2} spectrum), 2.2 – 5.6 (for an $E^{-2.5}$ spectrum) signal events per source in the full data taking period.

4. Results

After unblinding the data, there were on average 31 events observed inside the 5 degree cone around each candidate source. For each dataset in the 5° cone, the p-value (significance) is computed to determine whether or not the candidate source is significantly detected.

All candidate sources are consistent with a background-only hypothesis, i.e. no candidate source is significantly observed. The most signal-like sources are:

$E^{-2.0}$

δ (deg)	N_{sig} ref.flux	N_{bg}	med. λ_{H0}	sens. (N_{sig})	disc. (N_{sig})
-90	1.25	51.05	-0.91	3.13	3.96
-70	1.30	51.12	-0.95	3.05	3.82
-50	1.43	51.65	-1.07	2.90	3.30
-30	0.88	29.85	-0.65	2.68	3.17
-10	0.78	24.44	-0.58	2.70	2.88
10	0.72	28.00	-0.54	2.60	2.62
30	0.66	28.35	-0.51	2.47	2.26
50	0.51	21.98	-0.40	2.32	1.83
55	0.33	13.75	-0.26	2.24	1.59

$E^{-2.5}$

δ (deg)	N_{sig} ref.flux	N_{bg}	med. λ_{H0}	sens. (N_{sig})	disc. (N_{sig})
-90	13.18	51.05	-8.89	3.58	5.38
-70	13.17	51.12	-8.93	3.59	5.53
-50	12.91	51.65	-8.90	3.57	5.16
-30	9.02	29.85	-6.13	3.46	4.82
-10	7.65	24.44	-5.23	3.19	4.38
10	6.17	28.00	-4.28	3.21	3.87
30	4.65	28.35	-3.37	2.78	3.35
50	2.74	21.98	-2.05	2.62	2.66
55	1.74	13.75	-1.31	2.47	2.23

Table 1: Summary of the discovery potential and sensitivity for the reference fluxes: $\phi^{\cos}_{\nu_i+\bar{\nu}_i} = 1.2 = 1 \cdot 10^{-4} \left(\frac{E}{\text{GeV}}\right)^{-2}$ (top), $1.8 \cdot 10^{-1} \cdot \left(\frac{E}{\text{GeV}}\right)^{-2.5}$ (bottom), in GeV^{-1} cm^{-2} s^{-1}. Listed are the total number of signal events for the concerned reference flux and the number of background events inside the 5 degree cone represented by the analysed 2D histograms, and the medians of the H0 test statistic (λ) distribution with the resulting number of events needed for a 90% confidence level exclusion or a 3σ discovery.

- For the $E^{-2.0}$ spectrum: The AGN J1512-0905 at right ascension 228.21°, declination −9.10° with a pre-trial p-value of 0.011. The post-trial p-value for the E^{-2} analysis was 0.66.
- For the $E^{-2.5}$ spectrum: The BL Lac Mkn 421 at right ascension 166.11°, declination 38.21° with a pre-trial p-value of 0.020. The post-trial p-value for the $E^{-2.5}$ analysis was 0.56.
- For the $E^{-3.2}$ spectrum: NGC 1068 was the only source candidate studied. This active galactic nuclei is located at right ascension 40.7°, declination −0.01° ($\sin\delta = 0.00$) with a pre-trial p-value of 0.98. Since there was only one trial, the post-trial p-value for the $E^{-3.2}$ analysis is automatically also: 0.98.

Because no significant detection is made, upper limits are set on the flux. If λ_{obs} is below the median expected λ for the background-only test statistic distribution, $\lambda(\mu_{\text{true}} = 0)$ is used for the upper limit calculation. This means the limit will match with the sensitivity for such cases. The computed upper limits for each source are shown in Figure 3 together with the overall sensitivity.

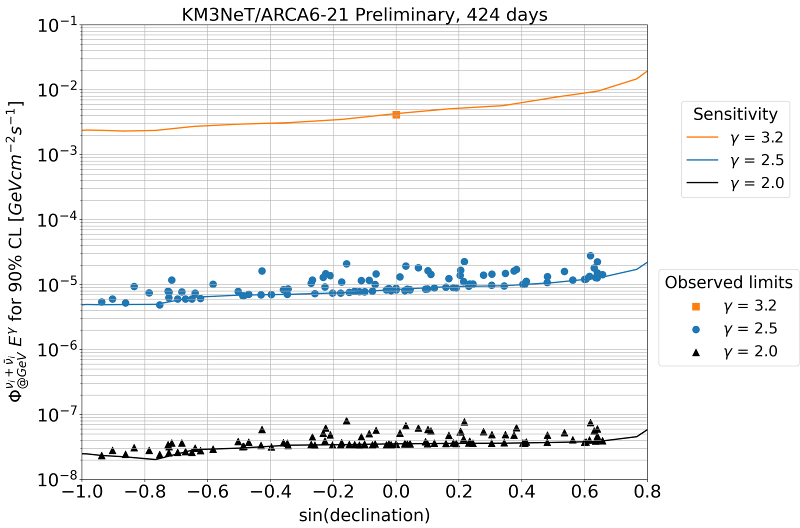

Figure 3: Sensitivity and observed limits for ARCA6-21 using 424 days of data. The γ = 2.0 and 2.5 analyses show the observed limits of 101 sources while the 3.2 analysis only looked at NGC 1068.

In Figure 4 the final ARCA6-21 E^{-2} point source results are compared with the IceCube and ANTARES experiments [11–13], as well as the previous ARCA point source analyses, and with the expected sensitivity for the full ARCA detector comprising 2 building blocks [8]. The improvement in sensitivity is expected to accelerate due to the planned deployment of 9 detection lines before the end of 2023 and another 9 months of unprocessed ARCA21 data.

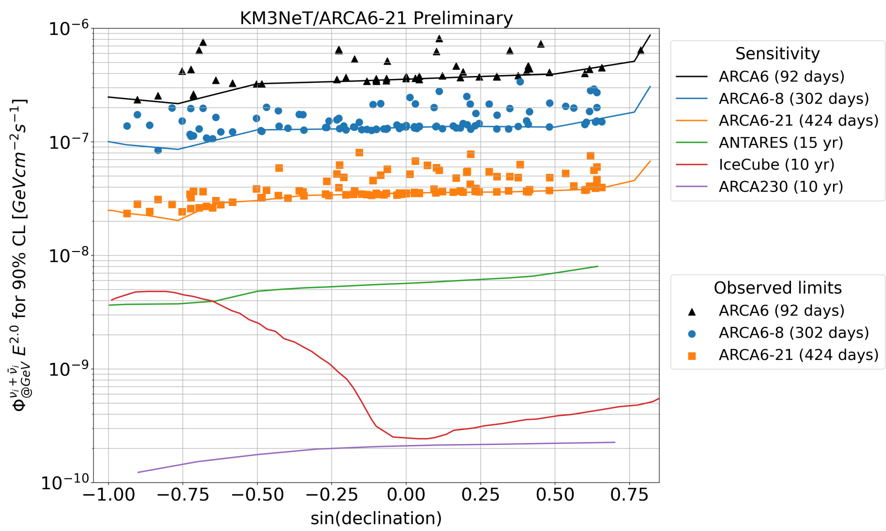

Figure 4: Comparison of the observed limits on the flux for the ARCA6-21 point source analysis assuming an E^{-2} source spectrum as a function of $\sin(\delta)$, with earlier presented results of ANTARES 15 years [11] and IceCube [12, 13], as well as the ARCA230 10 years sensitivity [8].

References

[1] IceCube Collaboration. GCN/AMON NOTICE 50579430_130033. Sept. 2017. url: https://gcn.gsfc.nasa.gov/notices_amon/50579430_130033.amon.

[2] IceCube Collaboration, MAGIC, AGILE, ASAS-SN, HAWC, HESS, ... & Kappesser, D. (2018). Multimessenger observations of a flaring blazar coincident with high-energy neutrino IceCube-170922A. Science, 361(6398), eaat1378.

[3] IceCube Collaboration (2018). Neutrino emission from the direction of the blazar TXS 0506+ 056 prior to the IceCube-170922A alert. Science, 361(6398), 147-151.

[4] IceCube Collaboration (2022). Evidence for neutrino emission from the nearby active galaxy NGC 1068. Science, 378(6619), 538-543.

[5] Aiello, S., Albert, A., Garre, S. A., et al. (2020). gSeaGen: The KM3NeT GENIE-based code for neutrino telescopes. Computer Physics Communications, 256, 107477.

[6] KM3NeT Collaboration. (2021). Upgrading gSeaGen: from MeV to PeV neutrinos. Journal of Instrumentation, 16(09), C09008.

[7] Carminati, G., Bazzotti, M., Margiotta, A., & Spurio, M. (2008). Atmospheric MUons from PArametric formulas: a fast GEnerator for neutrino telescopes (MUPAGE). Computer Physics Communications, 179(12), 915-923.

[8] Van Eeden, T. J. et al. (2023). Astronomy potential of KM3NeT/ARCA230. PoS(ICRC2023)1075.

[9] Fillipini, F. et al. (2023). Search for a diffuse astrophysical neutrino flux from the Galactic Ridge using KM3NeT/ARCA data. PoS(ICRC2023)1075.

[10] Tsourapis, V. et al. (2023). Search for a diffuse astrophysical neutrino flux with KM3NeT/ARCA using data of 2021-2022. PoS(ICRC2023)1195

[11] Alves, S. et al. (2023). Searches for point-like sources of cosmic neutrinos with the complete ANTARES dataset. PoS(ICRC2023)1128.

[12] Aartsen, M. G. et al. (2017). All-sky search for time-integrated neutrino emission from astrophysical sources with 7 yr of IceCube data. The Astrophysical Journal, 835(2), 151.

[13] Aartsen, M. G. et al. (2020). Time-integrated neutrino source searches with 10 years of IceCube data. Physical review letters, 124(5), 051103.

Full Authors List: The KM3NeT Collaboration

S. Aiello[a], A. Albert[b,bd], S. Alves Garre[c], Z. Aly[d], A. Ambrosone[f,e], F. Ameli[g], M. Andre[h], E. Androutsou[i], M. Anguita[j], L. Aphecetche[k], M. Ardid[l], S. Ardid[l], H. Atmani[m], J. Aublin[n], L. Bailly-Salins[o], Z. Bardačová[q,p], B. Baret[n], A. Bariego-Quintana[c], S. Basegmez du Pree[r], Y. Becherini[n], M. Bendahman[m,n], F. Benfenati[t,s], M. Benhassi[u,e], D. M. Benoit[v], E. Berbee[r], V. Bertin[d], S. Biagi[w], M. Boettcher[x], D. Bonanno[w], J. Boumaaza[m], M. Bouta[y], M. Bouwhuis[r], C. Bozza[z,e], R. M. Bozza[f,e], H.Brânzaş[aa], F. Bretaudeau[k], R. Bruijn[ab,r], J. Brunner[d], R. Bruno[a], E. Buis[ac,r], R. Buompane[u,e], J. Busto[d], B. Caiffi[ad], D. Calvo[c], S. Campion[g,ae], A. Capone[g,ae], F. Carenini[t,s], V. Carretero[c], T. Cartraud[n], P. Castaldi[af,s], V. Cecchini[c], S. Celli[g,ae], L. Cerisy[d], M. Chabab[ag], M. Chadolias[ah], A. Chen[ai], S. Cherubini[aj,w], T. Chiarusi[s], M. Circella[ak], R. Cocimano[w], J. A. B. Coelho[n], A. Coleiro[n], R. Coniglione[w] P. Coyle[d], A. Creusot[n], A. Cruz[al], G. Cuttone[w], R. Dallier[k], Y. Darras[ah], A. De Benedittis[e], B. De Martino[d], V. Decoene[k], R. Del Burgo[e], U. M. Di Cerbo[e], L. S. Di Mauro[w], I. Di Palma[g,ae], A. F. Díaz[j], C. Diaz[j], D. Diego-Tortosa[w], C. Distefano[w], A. Domi[ah], C. Donzaud[n], D. Dornic[d], M. Dörr[am], E. Drakopoulou[i], D. Drouhin[b,bd], R. Dvornický[q], T. Eberl[ah], E. Eckerová[q,p], A. Eddymaoui[m], T. van Eeden[r], M. Eff[n], D. van Eijk[r], I. El Bojaddaini[y], S. El Hedri[n], A. Enzenhöfer[d], G. Ferrara[w], M. D. Filipović[an], F. Filippini[t,s], D. Franciotti[w], L. A. Fusco[z,e], J. Gabriel[ao], S. Gagliardini[g], T. Gal[ah], J. García Méndez[l], A. Garcia Soto[c], C. Gatius Oliver[r], N. Geißelbrecht[ah], H. Ghaddari[y], L. Gialanella[e,u], B. K. Gibson[v], E. Giorgio[w], I. Goos[n], D. Goupilliere[o], S. R. Gozzini[c], R. Gracia[ah], K. Graf[ah], C. Guidi[ap,ad], B. Guillon[o], M. Gutiérrez[aq], H. van Haren[ar], A. Heijboer[r], A. Hekalo[am], L. Hennig[ah], J. J. Hernández-Rey[c], F. Huang[d], W. Idrissi Ibnsalih[e], G. Illuminati[s], C. W. James[al], M. de Jong[as,r], P. de Jong[ab,r], B. J. Jung[r], P. Kalaczyński[at,be], O. Kalekin[ah], U. F. Katz[ah], N. R. Khan Chowdhury[c], A. Khatun[q], G. Kistauri[av,au], C. Kopper[ah], A. Kouchner[aw,n], V. Kulikovskiy[ad], R. Kvatadze[av], M. Labalme[o], R. Lahmann[ah], G. Larosa[w], C. Lastoria[d], A. Lazo[c], S. Le Stum[d], G. Lehaut[o], E. Leonora[a], N. Lessing[c], G. Levi[t,s], M. Lindsey Clark[n], F. Longhitano[a], J. Majumdar[r], L. Malerba[ad], F. Mamedov[p], J. Mańczak[c], A. Manfreda[e], M. Marconi[ap,ad], A. Margiotta[t,s], A. Marinelli[e,f], C. Markou[i], L. Martin[k], J. A. Martínez-Mora[l], F. Marzaioli[u,e], M. Mastrodicasa[ae,g], S. Mastroianni[e], S. Miccichè[w], G. Miele[f,e], P. Migliozzi[e], E. Migneco[w], M. L. Mitsou[e], C. M. Mollo[e], L. Morales-Gallegos[u,e], C. Morley-Wong[al], A. Moussa[y], I. Mozun Mateo[ay,ax], R. Muller[r], M. R. Musone[e,u], M. Musumeci[w], L. Nauta[r], S. Navas[aq], A. Nayerhoda[ak], C. A. Nicolau[g], B. Nkosi[ai], B. Ó Fearraigh[ab,r], V. Oliviero[f,e], A. Orlando[w], E. Oukacha[n], D. Paesani[w], J. Palacios González[c], G. Papalashvili[au], V. Parisi[ap,ad], E.J. Pastor Gomez[c], A. M. Păun[aa], G. E. Păvălaş[aa], S. Peña Martínez[n], M. Perrin-Terrin[d], J. Perronnel[o], V. Pestel[ay], R. Pestes[n], P. Piattelli[w], C. Poirè[z,e], V. Popa[aa], T. Pradier[b], S. Pulvirenti[w], G. Quéméner[o], C. Quiroz[l], U. Rahaman[c], N. Randazzo[a], R. Randriatoamanana[k], S. Razzaque[az], I. C. Rea[e], D. Real[c], S. Reck[ah], G. Riccobene[w], J. Robinson[x], A. Romanov[ap,ad], A. Šaina[c], F. Salesa Greus[c], D. F. E. Samtleben[as,r], A. Sánchez Losa[c,ak], S. Sanfilippo[w], M. Sanguineti[ap,ad], C. Santonastaso[ba,e], D. Santonocito[w], P. Sapienza[w], J. Schnabel[ah], J. Schumann[ah], H. M. Schutte[x], J. Seneca[r], N. Sennan[y], B. Setter[ah], I. Sgura[ak], R. Shanidze[au], Y. Shitov[p], F. Šimkovic[q], A. Simonelli[e], A. Sinopoulou[a], M.V. Smirnov[ah], B. Spisso[e], M. Spurio[t,s], D. Stavropoulos[i], I. Štekl[p], M. Taiuti[ap,ad], Y. Tayalati[m], H. Tedjditi[ad], H. Thiersen[x], I. Tosta e Melo[a,aj], B. Trocmé[n], V. Tsourapis[i], E. Tzamariudaki[i], A. Vacheret[o], V. Valsecchi[w], V. Van Elewyck[aw,n], G. Vannoye[d], G. Vasileiadis[bb], F. Vazquez de Sola[r], C. Verilhac[n], A. Veutro[g,ae], S. Viola[w], D. Vivolo[u,e], J. Wilms[bc], E. de Wolf[ab,r], H. Yepes-Ramirez[l], G. Zarpapis[i], S. Zavatarelli[ad], A. Zegarelli[g,ae], D. Zito[w], J. D. Zornoza[c], J. Zúñiga[c], and N. Zywucka[x].

[a]INFN, Sezione di Catania, Via Santa Sofia 64, Catania, 95123 Italy
[b]Université de Strasbourg, CNRS, IPHC UMR 7178, F-67000 Strasbourg, France
[c]IFIC - Instituto de Física Corpuscular (CSIC - Universitat de València), c/Catedrático José Beltrán, 2, 46980 Paterna, Valencia, Spain
[d]Aix Marseille Univ, CNRS/IN2P3, CPPM, Marseille, France
[e]INFN, Sezione di Napoli, Complesso Universitario di Monte S. Angelo, Via Cintia ed. G, Napoli, 80126 Italy
[f]Università di Napoli "Federico II", Dip. Scienze Fisiche "E. Pancini", Complesso Universitario di Monte S. Angelo, Via Cintia ed. G, Napoli, 80126 Italy
[g]INFN, Sezione di Roma, Piazzale Aldo Moro 2, Roma, 00185 Italy
[h]Universitat Politècnica de Catalunya, Laboratori d'Aplicacions Bioacústiques, Centre Tecnològic de Vilanova i la Geltrú, Avda. Rambla Exposició, s/n, Vilanova i la Geltrú, 08800 Spain
[i]NCSR Demokritos, Institute of Nuclear and Particle Physics, Ag. Paraskevi Attikis, Athens, 15310 Greece
[j]University of Granada, Dept. of Computer Architecture and Technology/CITIC, 18071 Granada, Spain
[k]Subatech, IMT Atlantique, IN2P3-CNRS, Université de Nantes, 4 rue Alfred Kastler - La Chantrerie, Nantes, BP 20722 44307 France
[l]Universitat Politècnica de València, Instituto de Investigación para la Gestión Integrada de las Zonas Costeras, C/ Paranimf, 1, Gandia, 46730 Spain
[m]University Mohammed V in Rabat, Faculty of Sciences, 4 av. Ibn Battouta, B.P. 1014, R.P. 10000 Rabat, Morocco
[n]Université Paris Cité, CNRS, Astroparticule et Cosmologie, F-75013 Paris, France
[o]LPC CAEN, Normandie Univ, ENSICAEN, UNICAEN, CNRS/IN2P3, 6 boulevard Maréchal Juin, Caen, 14050 France
[p]Czech Technical University in Prague, Institute of Experimental and Applied Physics, Husova 240/5, Prague, 110 00 Czech Republic
[q]Comenius University in Bratislava, Department of Nuclear Physics and Biophysics, Mlynska dolina F1, Bratislava, 842 48 Slovak Republic
[r]Nikhef, National Institute for Subatomic Physics, PO Box 41882, Amsterdam, 1009 DB Netherlands
[s]INFN, Sezione di Bologna, v.le C. Berti-Pichat, 6/2, Bologna, 40127 Italy
[t]Università di Bologna, Dipartimento di Fisica e Astronomia, v.le C. Berti-Pichat, 6/2, Bologna, 40127 Italy
[u]Università degli Studi della Campania "Luigi Vanvitelli", Dipartimento di Matematica e Fisica, viale Lincoln 5, Caserta, 81100 Italy
[v]E. A. Milne Centre for Astrophysics, University of Hull, Hull, HU6 7RX, United Kingdom

[w]INFN, Laboratori Nazionali del Sud, Via S. Sofia 62, Catania, 95123 Italy
[x]North-West University, Centre for Space Research, Private Bag X6001, Potchefstroom, 2520 South Africa
[y]University Mohammed I, Faculty of Sciences, BV Mohammed VI, B.P. 717, R.P. 60000 Oujda, Morocco
[z]Università di Salerno e INFN Gruppo Collegato di Salerno, Dipartimento di Fisica, Via Giovanni Paolo II 132, Fisciano, 84084 Italy
[aa]ISS, Atomistilor 409, Măgurele, RO-077125 Romania
[ab]University of Amsterdam, Institute of Physics/IHEF, PO Box 94216, Amsterdam, 1090 GE Netherlands
[ac]TNO, Technical Sciences, PO Box 155, Delft, 2600 AD Netherlands
[ad]INFN, Sezione di Genova, Via Dodecaneso 33, Genova, 16146 Italy
[ae]Università La Sapienza, Dipartimento di Fisica, Piazzale Aldo Moro 2, Roma, 00185 Italy
[af]Università di Bologna, Dipartimento di Ingegneria dell'Energia Elettrica e dell'Informazione "Guglielmo Marconi", Via dell'Università 50, Cesena, 47521 Italia
[ag]Cadi Ayyad University, Physics Department, Faculty of Science Semlalia, Av. My Abdellah, P.O.B. 2390, Marrakech, 40000 Morocco
[ah]Friedrich-Alexander-Universität Erlangen-Nürnberg (FAU), Erlangen Centre for Astroparticle Physics, Nikolaus-Fiebiger-Straße 2, 91058 Erlangen, Germany
[ai]University of the Witwatersrand, School of Physics, Private Bag 3, Johannesburg, Wits 2050 South Africa
[aj]Università di Catania, Dipartimento di Fisica e Astronomia "Ettore Majorana", Via Santa Sofia 64, Catania, 95123 Italy
[ak]INFN, Sezione di Bari, via Orabona, 4, Bari, 70125 Italy
[al]International Centre for Radio Astronomy Research, Curtin University, Bentley, WA 6102, Australia
[am]University Würzburg, Emil-Fischer-Straße 31, Würzburg, 97074 Germany
[an]Western Sydney University, School of Computing, Engineering and Mathematics, Locked Bag 1797, Penrith, NSW 2751 Australia
[ao]IN2P3, LPC, Campus des Cézeaux 24, avenue des Landais BP 80026, Aubière Cedex, 63171 France
[ap]Università di Genova, Via Dodecaneso 33, Genova, 16146 Italy
[aq]University of Granada, Dpto. de Física Teórica y del Cosmos & C.A.F.P.E., 18071 Granada, Spain
[ar]NIOZ (Royal Netherlands Institute for Sea Research), PO Box 59, Den Burg, Texel, 1790 AB, the Netherlands
[as]Leiden University, Leiden Institute of Physics, PO Box 9504, Leiden, 2300 RA Netherlands
[at]National Centre for Nuclear Research, 02-093 Warsaw, Poland
[au]Tbilisi State University, Department of Physics, 3, Chavchavadze Ave., Tbilisi, 0179 Georgia
[av]The University of Georgia, Institute of Physics, Kostava str. 77, Tbilisi, 0171 Georgia
[aw]Institut Universitaire de France, 1 rue Descartes, Paris, 75005 France
[ax]IN2P3, 3, Rue Michel-Ange, Paris 16, 75794 France
[ay]LPC, Campus des Cézeaux 24, avenue des Landais BP 80026, Aubière Cedex, 63171 France
[az]University of Johannesburg, Department Physics, PO Box 524, Auckland Park, 2006 South Africa
[ba]Università degli Studi della Campania "Luigi Vanvitelli", CAPACITY, Laboratorio CIRCE - Dip. Di Matematica e Fisica - Viale Carlo III di Borbone 153, San Nicola La Strada, 81020 Italy
[bb]Laboratoire Univers et Particules de Montpellier, Place Eugène Bataillon - CC 72, Montpellier Cédex 05, 34095 France
[bc]Friedrich-Alexander-Universität Erlangen-Nürnberg (FAU), Remeis Sternwarte, Sternwartstraße 7, 96049 Bamberg, Germany
[bd]Université de Haute Alsace, rue des Frères Lumière, 68093 Mulhouse Cedex, France
[be]AstroCeNT, Nicolaus Copernicus Astronomical Center, Polish Academy of Sciences, Rektorska 4, Warsaw, 00-614 Poland

Acknowledgements

The authors acknowledge the financial support of the funding agencies: Agence Nationale de la Recherche (contract ANR-15-CE31-0020), Centre National de la Recherche Scientifique (CNRS), Commission Européenne (FEDER fund and Marie Curie Program), LabEx UnivEarthS (ANR-10-LABX-0023 and ANR-18-IDEX-0001), Paris Île-de-France Region, France; Shota Rustaveli National Science Foundation of Georgia (SRNSFG, FR-22-13708), Georgia; The General Secretariat of Research and Innovation (GSRI), Greece Istituto Nazionale di Fisica Nucleare (INFN), Ministero dell'Università e della Ricerca (MIUR), PRIN 2017 program (Grant NAT-NET 2017W4HA7S) Italy; Ministry of Higher Education, Scientific Research and Innovation, Morocco, and the Arab Fund for Economic and Social Development, Kuwait; Nederlandse organisatie voor Wetenschappelijk Onderzoek (NWO), the Netherlands; The National Science Centre, Poland (2021/41/N/ST2/01177); The grant "AstroCeNT: Particle Astrophysics Science and Technology Centre", carried out within the International Research Agendas programme of the Foundation for Polish Science financed by the European Union under the European Regional Development Fund; National Authority for Scientific Research (ANCS), Romania; Grants PID2021-124591NB-C41, -C42, -C43 funded by MCIN/AEI/ 10.13039/501100011033 and, as appropriate, by "ERDF A way of making Europe", by the "European Union" or by the "European Union NextGenerationEU/PRTR", Programa de Planes Complementarios I+D+I (refs. ASFAE/2022/023, ASFAE/2022/014), Programa Prometeo (PROMETEO/2020/019) and GenT (refs. CIDEGENT/2018/034, /2019/043, /2020/049. /2021/23) of the Generalitat Valenciana, Junta de Andalucía (ref. SOMM17/6104/UGR, P18-FR-5057), EU: MSC program (ref. 101025085), Programa María Zambrano (Spanish Ministry of Universities, funded by the European Union, NextGenerationEU), Spain; The European Union's Horizon 2020 Research and Innovation Programme (ChETEC-INFRA - Project no. 101008324).